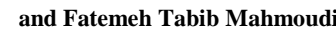


Earth Observation and Geomatics Engineering

Homepage: https://eoge.ut.ac.ir/

Short-Term Spatiotemporal Changes Analysis in Wetlands Areas (Case Study: MianKaleh Wetland)





Online ISSN: 2588-4360

- Navid Alizadeh ¹ and Fatemeh Tabib Mahmoudi² □

 1. Department of Geomatics Engineering, Faculty of Civil, Shahid Rajaee Teacher Training University, Tehran, Iran. E-mail: navidalz60@sru.ac.ir
- 2. Corresponding author, Department of Geomatics Engineering, Faculty of Civil, Shahid Rajaee Teacher Training University, Tehran, Iran. E-mail: fmahmoudi@sru.ac.ir

ABSTRACT Article Info

Article type:

Research Article

Article history:

Received 2025-05-20 Received in revised form 2025-06-27 Accepted 2025-07-24 Published online 2025-10-19

Keywords:

Change Detection, Wetlands, post-classification, Random Forest, Feature Fusion

Wetlands are important areas for several main reasons such as their ability to purify the air, having the main resources of income for the local people by attracting tourists and being habitats for various plant and animal species. Wetlands' drought causes major challenges such as biodiversity reduction, increasing soil erosion and dust, water pollution, unemployment and poverty. Remote sensing data is one of the best tools available for better managing and protection of wetland resources, as well as monitoring changes, due to its high accuracy, speed, and low cost compared to the field measurements.

This study examines the Land Use Land Cover (LULC) changes in the Miankaleh wetland in a short-term study composed of seven-year period between 2016 and 2023, using Sentinel-2 satellite images and a Digital Elevation Model (DEM). The proposed method is a postclassification change analysis based on the supervised Random Forest classifier and the spectral and elevation features fusion.

The obtained results of the changes analysis in the Miankaleh wetland represents that during the seven-year period studied in this research, the area of water bodies decreased by 6% and the area of barren lands increased by about 7% due to the wetland's drought. However, the rate of changes was more severe in the recent four years of this study (2019 to 2023) by decreasing the 11343.36 hectares of water bodies' area and increasing the 14102 hectares to the area of the barren lands.

The obtained change detection results in this short-term study represent the rapid rate of changing in the MianKaleh wetland region due to the drought of water bodies, in a seven-year period, and increasing the constructions and farming. Moreover, categorizing the time interval of this study into two parts of first three years (2016 to 2019) and last four years (2019 to 2023) showed that the rate of drying out of the wetland's water bodies has been increasing rapidly in recent four years with about 6 times more than the first three years.

Cite this article: Alizadeh, N., & Tabib Mahmoudi, F. (2025). Short-term Spatiotemporal Change Analysis in Wetlands Areas (Case Study: Miankaleh Wetland), Earth Observation and Geomatics Engineering, Volume 8, Issue 2, Pages 96-105. http//doi.org/10.22059/eoge.2025.395683.1178



© The Author(s).

DOI: http://doi.org/10.22059/eoge.2025.395683.1178

Publisher: University of Tehran.

1. Introduction

Nowadays, due to the human intervention in the ecosystem, numerous changes have occurred in the natural form of the earth, including changes in land use, vegetation, and natural resources (Anand, Gosain et al. 2018, Nasiri, Deljouei et al. 2022). Some changes occur due to natural causes, such as those caused by storms or wildfires, while other changes on the land, such as resource extraction. construction, and urban growth, result from human projects (Bayat and Mahmoudi 2022). Numerous environmental challenges, including the decline in groundwater levels, the expansion of agricultural lands, the uncontrolled urbanization and urban developments (Tabib Mahmoudi and Hosseini 2021), the loss of vegetation, and the drying of wetlands are among the most important human impacts on the environment (Matlhodi, Kenabatho et al. 2021). Understanding these changes and the threats they pose in sensitive areas such as wetlands is essential due to the presence of rare plant and animal species.

Wetlands are of great important areas for several main reasons, the most important of which are that these areas are habitats for various plant and animal species, they oxygenate the region and purify the air, and they are one of the main resources of income for the local people by attracting tourists and creating commercial areas. Therefore, climate change and environmental disasters, the consequent drying of wetlands and the loss of vegetation around them, in addition to their effects on nature and its inhabitants, also have social and economic consequences for local communities (Zahir, Thennakoon et al. 2021). Reduced biodiversity, increased soil erosion, water pollution, increased dust, unemployment, poverty, and migration are some of the consequences of wetlands' drought.

Predicting the process of wetlands' changes and recognizing the factors that cause them can prevent the destruction of wetland areas to a large extent. Remote sensing data are one of the best and most accurate tools for such monitoring applications (Eastman and Toledano 2018, Hu and Dong 2018, Toure, Stow et al. 2018, Karim Tabbahfar and Tabib Mahmoudi 2024). For instance, remote sensing data are used for determining the classes and the distribution of land cover in the Savannah River basin in South Carolina and Georgia (Zurqani, Post et al. 2018). Moreover, multi-temporal Landsat images from 1987 to 2017 are used for analyzing the land-cover changes in the central region of the lower Yangtze River using the random forest classification algorithm (Zhang and Zhang 2020). Based on the obtained time-series land-cover classification results, the spatiotemporal land-use/cover changes were analyzedLetta et al., performed a spatiotemporal changes detection in LULC for the years 1990, 2005, and 2019 from Landsat time series in the Chalus watershed using the maximum likelihood algorithm. Then, by the Land Cover Change Modeler, they predicted and modeled LULC changes for the years 2035 and 2050 (Leta, Demissie et al. 2021). Teshager et al., also analyzed LULC changes in the Kility watershed using Landsat images from 1986 and 2002 and Sentinel-2 images from 2019. They used the maximum likelihood algorithm to generate LULC maps (Teshager and Abeje 2021).

The results of extensive researches conducted in different wetland areas based on using various kinds of remote sensing data indicate a decrease in the area of wetlands in all around the world (Tian, Zhang et al. 2016, Wingate, Phinn et al. 2016, Khoshnood Motlagh, Sadoddin et al. 2021). The reason is that almost all of the investigated wetland areas have undergone destructive changes by human in addition to natural factors and climate change. For instance, the Bi-SRUNet++ deep learning algorithm is proposed for detecting the changes in Dongting Lake wetland in China and analyzed the trends of monthly predictions of NDVI and NDWI those are derived from Landsat-8 satellite images from 2021 to 2022 (Pan, Lin et al. 2023). Also, Pan, Xu, et al., proposed a change detection method in which multitemporal GaoFen images are used STANet model for spatial-temporal analyzing the Sanjiang National Nature Reserve area. Two images from GF-6 and GF-1 are utilized and compared with three band selection methods; RGB combination, principal component analysis and Relief F are compared to improve the changes detection of wetland surrounding area. The results depicts that the accuracy of the obtained results is related to various combinations of spectral bands and STANet models (Pan, Xu et al. 2022).

With the objective of using remote sensing technology for identifying the neglected wetlands in Pakistan, supervised classification and TCW are used. QuickBird imagery and Sentinel-2 satellite data from 2016 to 2019 were used for the changes analysis. Moreover, ASTER DEM was used for performing watershed analysis (Aslam, Shu et al. 2024). Baker, Lawrence et al., used Landsat images from 1988 and 2001 to detect the changes in the Gallatin Valley of southwest Montana as a wetland ecosystem. Stochastic gradient boosting (SGB) was used for classifying the 2001 image, and change vector analysis (CVA) was used for identifying the changes locations of wetland areas between 1988 and 2001(Baker, Lawrence et al. 2007).

Zhang, Wu el al., proposed an object-oriented change detection which creates classification rules based on decision tree method. This study is performed in 35 years, which is divided into five periods: 1980s, 1990s, 2000s, 2010s and 2015s and Landsat satellite images are used for dynamic change analysis of coastal wetland of the Pearl River (Zhang, Wu et al. 2021). In another research, the long-term changes are investigated in wetlands vegetation in Eastern Georgian Bay using the IKONOS images acquired in 2002–2003 and KOMPSAT-3 and Pleiades1A/1B images in 2019. The object based classification is used to map land cover in two periods, followed by monitoring the changes (Rupasinghe and Chow-Fraser 2024).

Bhattacharjee, Islam et al., investigated the LULC changes from 1989 to 2019 in the Haor area by using Landsat satellite images and performing an unsupervised classification algorithm to classify multi-temporal images

into five major classes using threshold values of MNDWI and NDVI indices. This study reveals that this area lost 489.6 ha (8.34%) of vegetation and 2208.6 ha (37.54%) of the deep waters among the last three decades (Bhattacharjee, Islam et al. 2021).

According to the research background, regular and short-term monitoring of wetland areas has an important role in protecting the ecosystem and preventing its destruction. In this regard, the main objective of this study is to examine the rate of changes of the LULC objects in the Miankaleh wetland in Mazandaran province, Iran, using multi-temporal satellite images. The main contribution of this research is to evaluate the rate of urbanization, agricultural changes, deforestation, and the area of water bodies in the MianKaleh wetland in a short-term study. By analyzing these changes, a solution can be presented for protecting the ecosystem of this valuable wetland.

2. Study Area and Datasets

The study area of this research is the Miankaleh Wetland in Mazandaran Province, Iran, which is bordered by the Caspian Sea from the north, and by the three cities of Behshahr, Bandar Turkman, and Bandar Gaz from the east and south, and by the Amirabad region and the industrial fishery zone from the west (Figure 1). This wetland has an area of more than 68000 hectares and its height is 15 to 28 meters below the sea level, and constitutes about 2.8% of the area of Mazandaran Province. The Miankaleh Wetland and its surrounding areas had many changes in recent years due to various reasons, including the reduction of the wetland's water area, an uncontrolled increase in constructions, deforestation and converting forests into other LULC classes.



Figure 1. Miankaleh wetland as the study area

In this research, three Sentinel-2 satellite images from 2016, 2019, and 2023 were used for LULC classification and changes analysis in the Miankaleh Wetland Basin. The time series of Sentinel-2 satellite images used in this study were acquired in the same month for each year to avoid reflectance differences and errors in the classification of each of the LULC object classes. The The Shuttle Radar Topography Mission (SRTM) digital elevation model was also used to improve the accuracy of the classification maps.

3. Methodology

The main objective of this study is to investigate the

performed changes in the Miankaleh Wetland and its surrounding areas using multi-temporal Sentinel-2 satellite images and SRTM digital elevation model. A post-classification change analysis algorithm is used for analyzing the changes in LULC objects within the Miankaleh Wetland. As illustrated in Figure 2, the proposed post-classification change detection method in this study consists of several key stages: data acquisition and preprocessing, LULC map generation composed of the feature extraction and performing Random Forest classifier, and post-classification change analysis.

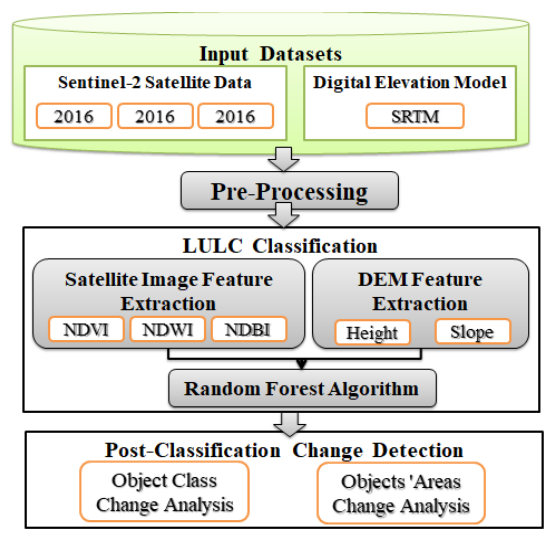


Figure 2. The structure of the proposed change analysis method

3.1. Data Acquisition and Pre-processing

Sentinel-2 Level-2A imagery for the selected years was obtained from the Google Earth Engine (GEE) platform. These images are atmospherically corrected and surface reflectance ready, ensuring high radiometric and geometric quality. Images were selected from the same seasonal period (late summer to early autumn) to minimize the phenological differences and atmospheric variability. Pre-processing involved the following steps:

- Cloud Masking: Scenes with less than 10% cloud cover were selected, and cloud pixels were masked using the Sen2Cor cloud probability layer.
- Radiometric Calibration: Surface reflectance values were confirmed to ensure uniform spectral data across the years.
- DEM Integration: SRTM DEM was used to derive topographic variables such as elevation and slope, which were resampled to match Sentinel-2's ten meters resolution.

3.2. LULC Classification Maps

In this research, the Random Forest classifier as a pixelbased method is used to classify each of the images into the object classes available in the study area. The Random Forest classifier is a supervised machine learning algorithm of ensemble learning methods that consist of a set of decision trees and their predictions are aggregated to identify the most popular result. In this ensemble method, a number of decision trees are located in various subsets of the dataset and their results are averaged for improving the prediction accuracies of dataset. In Random Forest algorithm, instead of using the results of one decision tree, the machine learning algorithm predicts the results from each tree based on the majority voting and takes the final result as the output. Using the results of multiple trees in the forest lead to higher accuracy and avoid the problem of over-fitting (Gall, Razavi et al. 2012, Talla, Venigalla et al. 2019).

3.3. Feature Generation and Fusion

Given that the processing steps are performed in the cloud environment of the GEE platform and the processing speed is very high, to improve the classification accuracy, some of the indices were calculated and added as additional bands to the satellite image bands:

1) Normalized Difference Vegetation Index (NDVI) to identify vegetative cover.

$$NDVI = (NIR - Red)/(NIR + Red)$$
 (1)

Where, NIR is the near infrared band of the Sentinel-2 satellite images.

2) Normalized Difference Water Index (NDWI) to delineate water bodies according to equation 2.

$$NDWI = (NIR - SWIR)/(NIR + SWIR)$$
 (2)

3) Normalized Difference Built-up Index (NDBI) to detect urban and impervious surfaces based on equation 3.

$$NDBI = (SWIR - NIR)/(SWIR + NIR)$$
 (3)

4) **Topographic features**: Elevation and slope layers derived from the DEM.

These spectral indices and topographic variables were stacked with the original Sentinel-2 bands to form a feature-rich input dataset for the classifier. This feature-level fusion enhances class separability, especially in ecologically heterogeneous regions like wetlands. Moreover, Fusion of these spectral and height indices with satellite image bands, in addition to facilitating classification, eliminates much of the noise introduced into the classification, thereby increasing the accuracy of the classification (Addae and Oppelt 2019).

After performing feature extraction from satellite images and DEM, the classification process by Random Forest classifier involved:

 Training Data Collection: Training samples for each LULC class were manually digitized using high-resolution imagery from Google Earth and expert knowledge of the region.

- 2) Classifier Parameterization: The RF classifier was configured with 100 trees and a maximum depth of 25. The number of features considered for splitting at each node was set to the square root of the total number of input features.
- 3) Model Training and Validation: For each year (2016, 2019, and 2023), the classifier was trained independently. Accuracy assessments were performed using independent validation samples and confusion matrices to compute overall accuracy and Kappa coefficients.

3.4. Post-Classification Change Analysis

After performing classification using the Random Forest algorithm on each of the satellite images taken from the study area, while comparing the classification maps of each year, the changes are analyzed. For post-classification change analysis in this research, following steps were undertaken:

- Change Matrix Generation: A change matrix (also known as a transition matrix) was created to identify transitions between different LULC classes across the years.
- **Temporal Comparison**: Two change intervals were analyzed 2016 to 2019 (3 years), and 2019 to 2023 (4 years) to identify both gradual and abrupt changes.
- Spatial Mapping of Change: Spatial overlays were used to visualize and quantify changes, highlighting hotspots of deforestation, urban sprawl, vegetation loss, and wetland shrinkage.

The analysis of changes occurred in the area of Miankaleh Wetland is presented with the following three points of view: 1) Analyzing the impact of deficiencies in the wetland's water area. 2) Analyzing the significant deforestations in this region as well as the loss of vegetation and shrubs in this wetland area. 3) Analyzing the urbanization, uncontrolled constructions and land deformation in recent years.

4. Experimental Results

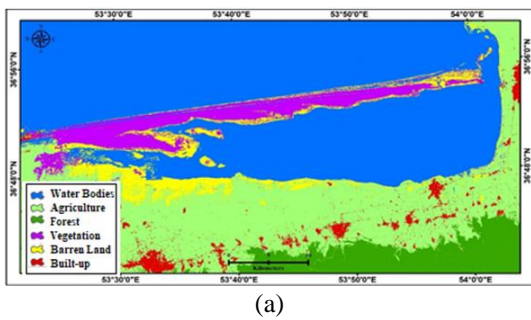
In order to evaluate the capabilities of the proposed change detection method in this research, Sentinel-2 satellite images taken from the Miankaleh wetland and its surrounding areas in 2016, 2019, and 2023 together with DEM were classified into six object classes according to Table 1. The generated classification maps by the Random Forest algorithm are illustrated in Figure 3.

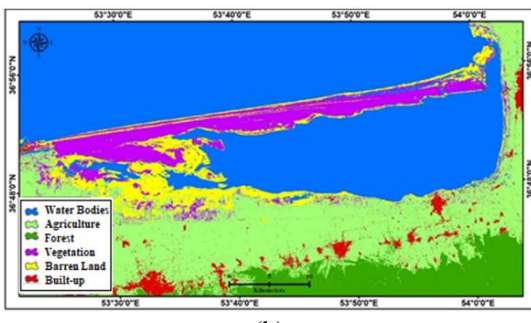
Table 1. LULC object classes and their descriptions

Object Class	Description
Forest	Broadleaf and coniferous trees
Agriculture	Irrigated, rained croplands
Vegetation	Grassland
Water Bodies	Continental water surfaces such as lake,
	wetlands, dam, and river
Barren Land	Bare soil and rocky mountains

Built-up Urban, suburban and rural areas

The areas of each of the LULC object classes and their changes in 2016, 2019 and 2023 are shown in Table 2. According to the results, the area percentage of water bodies in the study area has decreased from 47.01% to 41.25% from 2016 to 2023, and the area percentage of agricultural land has increased from 29.33% to 29.58% during this period.





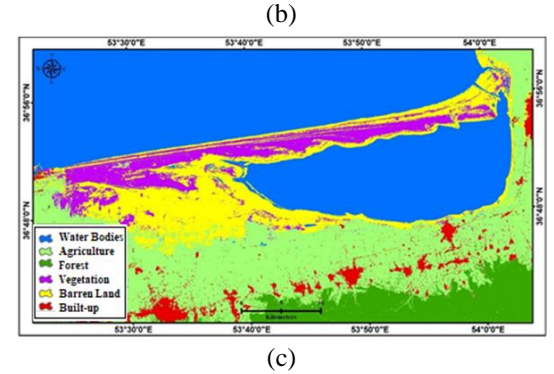


Figure 3. LULC classification maps of a) 2016, b) 2019 and c) 2023

Also, the area percentages of forest and vegetation classes have decreased from 8.95% to 8.09%, and 7.04% to 5.75%, respectively. The area percentages of barren land and built-up have increased from 5.08% to 12.13% and 2.58% to 3.19%, respectively. The most changes have been occurred in water bodies and barren land classes due to drought of this wetland.

According to the performed quantitative, semantic and visual analysis of total area changes in each of the object classes during this research period, some interpretations can be summarized:

 11500 ha of water bodies likely dried and turned into barren land.

- Around 800 ha of water bodies became agricultural land.
- 1600 ha of vegetation was lost mostly to barren land, and 401 ha to built-up areas.
- 578 ha increase in agriculture came from multiple classes (vegetation, forest, and water bodies).
- Barren land grew by 16383 ha, mostly from water, vegetation, and forest.
- Built-up areas expanded by 1440 ha, mainly from vegetation and agriculture.

Table 2. Area changes of the object classes

LULC	Area					
Object	2016	2019	2023	Total	Total	
Classes				Changes	Chang	
				(ha)	es (%)	
Water	109328.04	107275.16	95931.8	-13396.24	-5.76%	
Bodies	ha 47.01%	ha 46.13%	ha 41.25%			
Agricu	68211.76	68668.76	68790.3	+578.6	+0.25%	
lture	ha 29.33%	ha 29.53%	6 ha 29.58%			
Forest	20817.24	20321.04	18812.8	-2004.4	-0.86%	
	ha	ha	4 ha			
	8.95%	8.74%	8.09%			
Vegeta	16366.08	16064.8	13364.6	-3001.44	-1.29%	
tion	ha 7.04%	ha 6.91%	4 ha 5.75%			
Barren	11820 ha	14100.68	28203.0	+16383.0	+7.05	
Land	5.08%	ha 6.06%	4 ha 12.13%	4	%	
Built-	5993.64	6106.32	7434.08	+1440.44	+0.61%	
up	ha 2.58%	ha 2.62%	ha 3.19%			
Total	232536.76	232536.76	232536.	-	-	
Areas	ha	ha	76 ha			

Figures 4 and 5 compare the changes in the area of each of the defined object classes in the Miankaleh Wetland study area in 2016, 2019, and 2023. Some of the changed regions are highlighted by the red box in classification maps. Also, Figure 6 compares the positive or negative changes in the area of all object classes in 2016-2019 and 2019-2023 time intervals in a chart bar. As it can be seen, the water bodies, vegetation and forest have negative changes during the years 2016 to 2023. On the other hand, barren land, built-up and agriculture have positive changes in their areas during this study. Moreover, the rate of water body's reduction and increasing the barren lands in the second time interval of this study (2019-2023) is faster than the 2016-2019 time intervals.

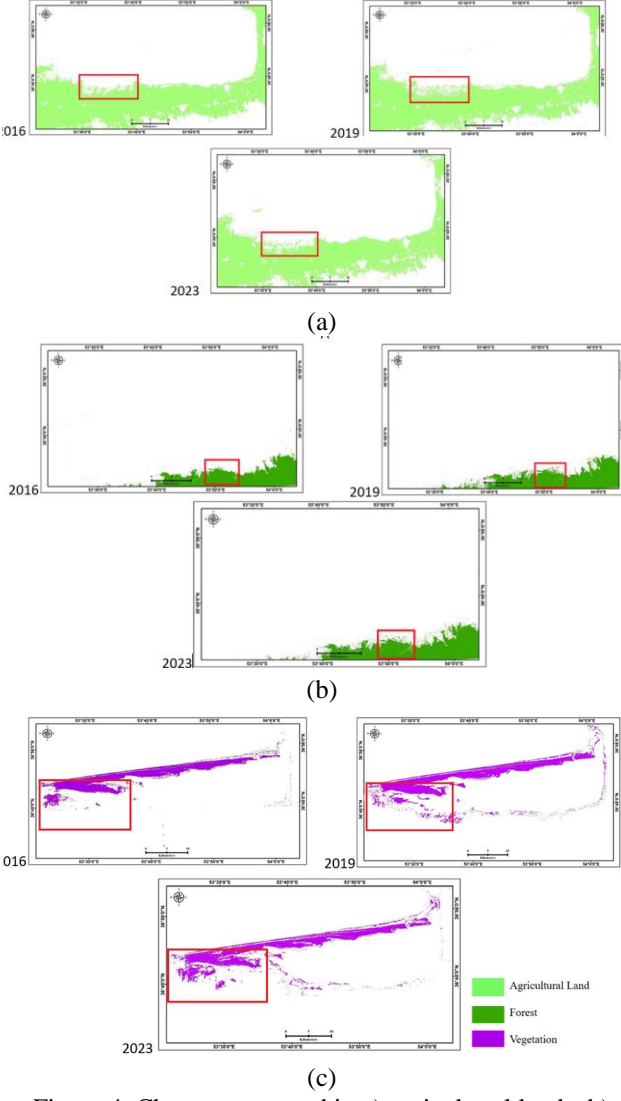
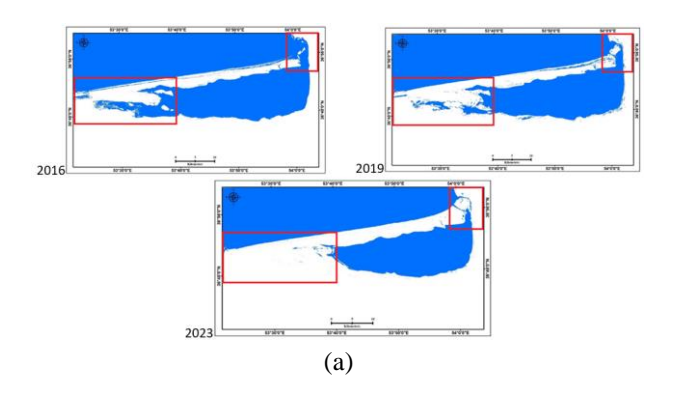


Figure 4. Changes occurred in a) agricultural lands, b) forest and c) vegetation between the years 2016, 2019 and 2023 (red boxes highlight some changes)



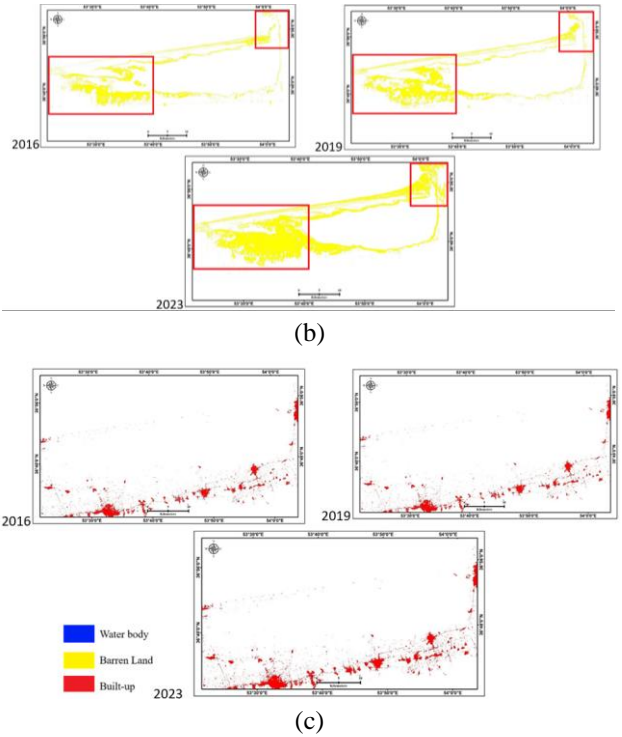


Figure 5. Changes occurred in a) water body, b) barren land and c) built-up between the years 2016, 2019 and 2023 (red boxes highlight some changes)

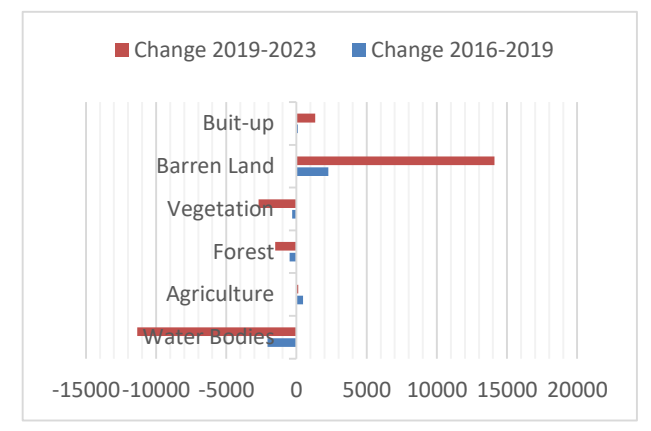


Figure 6. Positive and negative changes in the areas of each of the object classes

Figure 7 illustrates the total changes those were occurred in each of the LULC object classes during the years 2016 to 2023. Table 3 shows the full change matrix between all of the LULC object classes during 2016 to 2023.

Considering that part of the changes occurring in the Miankaleh Wetland area may be due to climate change phenomena such as global warming and variations in rainfall patterns, annual rainfall and temperature data for this region in the years 2016, 2019, and 2023 were analyzed to better interpret the obtained results of the change detection in the study area.

Table 3. LULC Change Matrix (2016–2023) in Hectares							
From \ To	Forest	Agriculture	Vegetation	Water Bodies	Barren Land	Built-up	Total (2016)
Forest	17289.6	1120.8	843.6	652.2	790.0	121.0	20817.2
Agriculture	954.0	61491.6	1123.2	1845.6	2805.6	991.8	68211.8
Vegetation	477.0	1120.8	11561.2	560.4	2433.6	213.1	16366.1
Water Bodies	289.8	804.6	450.0	88979.4	11500.2	1304.0	109328.0
Barren Land	101.2	339.0	142.0	271.6	10593.0	373.2	11820.0
Built-up	70.6	214.2	94.8	125.2	81.6	5407.2	5993.6
Total (2023)	18812.8	68790.4	13364.6	95931.8	28203.0	7434.1	232536.8

S3'300°E S3'400°E S3'500°E S4'00°E S4'00°E S4'00°E



Figure 7. LULC Change map from 2016 to 2023

Considering the fluctuations in precipitation over these years, it can be concluded that the Miankaleh Wetland region and Mazandaran Province are experiencing climate changes that are affecting rainfall patterns. These fluctuations can have direct impacts on water resources, agriculture, and local ecosystems. Moreover, temperature data also indicate an increasing trend in the average temperature of Mazandaran Province during the mentioned years. This rise in temperature can have significant effects on local ecosystems, water resources, and agriculture in the region.

Based on the available data, the average precipitation in Mazandaran province during the November–December for the years 2016, 2019, and 2023 is as Table 4. Moreover, according to meteorological data, the average temperature in Mazandaran Province during November–December for the years 2016, 2019, and 2023 is presented in Table 5.

Table 4. Rainfall analysis during the short-term study

Year	The cumulative rainfall of the rivers (mm)	Average Precipitatio n Volume (miliomm ³)	Change Compared to Last 2 Years (%)
2016	223	5829	-7
2019	263	6874	+35
2023	237	6179	+11

Table 5. Temperature analysis during the short-term study

Year	Average Temperature (°C)	Change Compared to Long-Term Average (4.4°C)
2016	Approximately 5.6	+1.2°C
2019	Approximately 7.0	+2.6°C
2023	Approximately 8.5	+4.1°C

As the change detection method in this research is the post-classification method, the user accuracy and producer accuracy of each of the object classes and the overall accuracies and Kappa coefficients of each of the LULC classification maps are utilized for evaluating the obtained change detection results. Tables 6 to 8 depicts the quantitative values of the accuracy assessments for the classification maps of the years 2016, 2019 and 2023, respectively.

Table 6. Accuracy assessment of the LULC classification map of

2016					
Class	User Accuracy (%)	Produce Accuracy (%)	Overall Accuracy (%)	Kappa Coefficient	
Forest	91.7	92.6	91	0.88	
Agriculture	93.5	92.9	91	0.88	

¹ https://www.mzrw.ir/st/198

Vegetation	92.5	86.0
Water	99.3	97.9
Bodies	99.3	21.2
Barren	92.2	95.0
Land	92.2	93.0
Built-up	96.8	95.8

Table 7. Accuracy assessment of the LULC classification map of

Class	User Accuracy	Produce Accuracy	Overall Accuracy	Kappa Coefficient
	(%)	(%)	(%)	
Forest	96.8	95.8	93	0.89
Agriculture	95.7	94.3		
Vegetation	94.8	91.0		
Water	98.6	98.6		
Bodies				
Barren	97.0	97.0		
Land				
Built-up	96.9	97.9		

Table 8. Accuracy assessment of the LULC classification map of 2023

Class	User Accuracy (%)	Produce Accuracy (%)	Overall Accuracy (%)	Kappa Coefficient
Forest	91.6	91.6	92	0.88
)2	0.00
Agriculture	92.9	93.6		
Vegetation	94.6	88.0		
Water	98.6	97.2		
Bodies				
Barren	95.0	96.0		
Land				
Built-up	97.9	97.9		

5. Discussion

Based on the comparison of the results of LULC classification maps for each of the years 2016, 2019, and 2023 in the Miankaleh wetland and its surrounding, the most obvious result of change detection points to about 6% decrease in the area of the water bodies in the short-term seven-year period studied. On the other hand, the area of barren lands, which are mostly created as a result of the drying the wetlands' water, has increased by about 7%. In addition, the reduction in vegetation cover around the wetland by 1.29% and the reduction in forest area by 0.81% are also important as the results of changes detection in the area of the Miankaleh wetland.

In some environmental studies conducted in recent years, deforestation with the aim of increasing construction in wetland areas has been cited as one of the effective factors in the drying up of wetland water bodies. Analysis of the results of this study also confirms the increase in constructions in this area by 0.69% in a short period of seven years.

Analysis of the trend of changes in the Miankaleh Wetland study area over a seven-year period of this research shows that the rate of decrease in the area of water bodies in the earlier four-year period between 2019 and 2023 is much faster than the rate of changes in the former three-year period (2016 to 2019). In other words, in the first three-year

period, the area of water bodies decreased by only 2,052.88 hectares, but in the second four-year period, this reduction reached 11,343.36 hectares, which has increased about 6 times. Similarly, the area of barren lands increased by only 2,280.68 hectares in the first three-year period (2016 to 2019), but in the second four-year period of the study, this increase reached 14,102.36 hectares. One of the reasons for this faster rate of drying of the wetlands can be attributed to the global warming and fluctuations in precipitation patterns.

In addition to water bodies and barren land, in other classes, the area changes were greater in the second fouryear period of the study compared to the first three-year period. For instance, the area of forests is decreased by only 496.2 hectares between 2016 and 2019, but in the period 2019 to 2023, this decrease in area reached 1508.2 hectares. In the built-up object class, the area changes in the second four-year period of the study were 1327.76 hectares and in the first three-year period were only 112.68 hectares. The increasing rate in the changes of the built-up class indicates the fast construction and urbanization. Moreover, according to the quantitative, semantic and visual analysis of total area changes in each of the object classes, some interpretations can be summarized: most areas of water bodies dried and turned into barren land, and in parallel, some areas of water bodies became agricultural land for food supply. 1600 ha of vegetation was lost mostly to barren land, and 401 ha to built-up areas. Built-up areas expanded by 1440 ha, mainly from vegetation and agriculture.

The statistical comparison of climatic variables with LULC transformations highlights a strong temporal alignment between increased temperature and decreased precipitation with the expansion of barren land and reduction of water bodies. Specifically, during the 2019-2023 interval, the mean temperature increased by approximately 1.5°C and precipitation declined by 10.1% compared to 2019, which coincides with a dramatic 11,343 ha (10.6%) reduction in water bodies and a 14,102 ha (100%) surge in barren land area. This correlation suggests a statistically significant linkage (Pearson's r \approx -0.92) between rising temperatures and wetland surface water loss. Simultaneously, built-up areas increased by 1,327 ha in the same period, primarily due to expanding tourism infrastructure and informal settlements driven by population pressures and land speculation near the wetland periphery. These trends imply that climate-induced stressors are compounded by unregulated human activities such as deforestation for fuelwood and illegal agriculture, accelerating ecosystem degradation. Hence, both climatic variability and anthropogenic interventions jointly drive LULC changes in Miankaleh, underscoring the urgent need for integrated land and climate governance.

The LULC change trends observed in the Miankaleh Wetland—most notably the 5.76% reduction in water bodies and a corresponding 7.05% increase in barren lands over a seven-year period—mirror the degradation patterns identified in other wetlands globally. For instance, similar

declines in aquatic and vegetated areas were reported in Dongting Lake, China, where NDVI and NDWI analyses revealed significant wetland shrinkage between 2021 and 2022 due to both anthropogenic and climatic stressors (Pan. Lin et al. 2023). Likewise, in Bangladesh's Haor region, a three-decade study noted a 37.54% decrease in deep water and an 8.34% loss in vegetation cover, driven by unsupervised agricultural expansion and hydrological regimes (Bhattacharjee, Islam et al. 2021). Furthermore, studies in the Sanjiang National Nature Reserve and Eastern Georgian Bay wetlands also indicated major transitions from natural cover types to barren or developed land, reflecting intensified urban encroachment and climate-induced vegetation stress (Pan, Xu et al. 2022, Rupasinghe and Chow-Fraser 2024). Compared to these regions, Miankaleh's rapid transformation, especially during the 2019-2023 interval, underscores an urgent convergence of human-induced pressure and climate variability. This comparative perspective not only validates the Miankaleh findings but also highlights the broader vulnerability of wetland ecosystems under compounding environmental pressures.

6. Conclusion

The post-classification change detection algorithm based on Random Forest classifier is applied on multi-temporal Sentinel-2 satellite images and SRTM DEM for short-term investigating the MianKaleh wetland. In recent years, many changes have been occurred in the study area of this research due to various factors such as the reduction of the wetland's water and the increase in barren lands due to the drought, increased construction, deforestation in the surrounding forests, and the increase in agricultural land. The obtained change detection results in this short-term study represent the rapid rate of changing in the MianKaleh wetland region due to the drought of water bodies, for about 6% in a seven-year period, and increasing the constructions and farming. Categorizing the time interval of this study into two parts of first three years (2016 to 2019) and last four years (2019 to 2023) showed that the rate of drying out of the wetland's water bodies and the increase in barren lands has been increasing rapidly in recent four years with about 6 times more than the first three years.

This study has demonstrated the high efficiency of remote sensing data in modeling land use and land cover changes, and the resulting maps can help executive managers make better decisions regarding the future of the Miankaleh Wetland Basin, preserve resources, and prevent further degradation.

LULC changes in wetlands has widespread negative consequences, including loss of biodiversity, reduced water quality, increased flood risk, greenhouse gas emissions, damage to the livelihoods of local communities, and high restoration costs. Therefore, short-term monitoring of wetlands for protection and preventing land use changes in these areas is of particular importance. According to the results of this study, if current negative rate of changes

continues; severe land degradation in the region is inevitable in the near future. Therefore, stakeholders such as local authorities or environmental managers should perform major activities for protecting the wetlands' area. One of these activities is strengthen monitoring and research by 1) Implementing regular environmental monitoring of water quality, species diversity, and habitat condition, 2) Use remote sensing and GIS mapping to detect changes in wetland extent and health, 3) Support research on climate change impacts, biodiversity trends, and restoration techniques to inform adaptive management.

Data Availability Statement

The datasets generated during and/or analyzed during the current study are available from the corresponding author on reasonable request.

Acknowledgment

This work was supported by Shahid Rajaee Teacher Training University under grant number 1404/394107.

References

- Addae, B. and N. Oppelt (2019). "Land-use/land-cover change analysis and urban growth modelling in the Greater Accra Metropolitan Area (GAMA), Ghana."

 <u>Urban Science</u> 3(1): 26.

 https://doi.org/10.3390/urbansci3010026.
- Anand, J., et al. (2018). "Prediction of land use changes based on Land Change Modeler and attribution of changes in the water balance of Ganga basin to land use change using the SWAT model." Science of the total environment 503-519. https://doi.org/10.1016/j.scitotenv.2018.07.017.
- Aslam, R. W., et al. (2024). "Wetland identification through remote sensing: insights into wetness, greenness, turbidity, temperature, and changing landscapes." <u>Big Data Research</u> 35: 100416. https://doi.org/10.1016/j.bdr.2023.100416.
- Baker, C., et al. (2007). "Change detection of wetland ecosystems using Landsat imagery and change vector analysis." Wetlands 27(3): 610-619, 10.1672/0277-5212(2007)27[610:CDOWEU]2.0.CO;2.
- Bayat, S. and F. T. Mahmoudi (2022). "Object Based Analysis of Land Use/Land Cover Changes Caused by Construction: A Case Study in the Mehr Pardis Housing Area." J. RS. GEOINF. RES. 1(1): 1-10, Winter & Spring 2023.
- Bhattacharjee, S., et al. (2021). "Land-use and land-cover change detection in a north-eastern wetland ecosystem of Bangladesh using remote sensing and GIS techniques." <u>Earth Systems and Environment</u> **5**(2): 319-340. https://doi.org/10.1007/s41748-021-00228-3.
- Eastman, J. R. and J. Toledano (2018). "A short presentation of the Land Change Modeler (LCM)." <u>Geomatic approaches for modeling land change scenarios</u>: 499-505. 10.1007/978-3-319-60801-3_36.
- Gall, J., et al. (2012). An introduction to random forests for multi-class object detection. Outdoor and Large-Scale Real-World Scene Analysis: 15th International Workshop

- on Theoretical Foundations of Computer Vision, Dagstuhl Castle, Germany, June 26-July 1, 2011. Revised Selected Papers, Springer. 10.1007/978-3-642-34091-8_11.
- Hu, Y. and Y. Dong (2018). "An automatic approach for land-change detection and land updates based on integrated NDVI timing analysis and the CVAPS method with GEE support." ISPRS journal of photogrammetry and remote sensing 146: 347-359. https://doi.org/10.1016/j.isprsjprs.2018.10.008.
- Karim Tabbahfar, H. and F. Tabib Mahmoudi (2024).

 "Optimum Spectral Indices for Water Bodies Recognition
 Based on Genetic Algorithm and Sentinel-2 Satellite
 Images." Journal of Electrical and Computer Engineering
 Innovations (JECEI) 12(1): 217-226.

 https://doi.org/10.22061/jecei.2023.10118.678.
- Khoshnood Motlagh, S., et al. (2021). "Analysis and prediction of land cover changes using the land change modeler (LCM) in a semiarid river basin, Iran." <u>Land Degradation & Development</u> **32**(10): 3092-3105. DOI: 10.1002/ldr.3969
- Leta, M. K., et al. (2021). "Modeling and prediction of land use land cover change dynamics based on land change modeler (Lcm) in nashe watershed, upper blue nile basin, Ethiopia." <u>Sustainability</u> **13**(7): 3740. https://doi.org/10.3390/su13073740.
- Matlhodi, B., et al. (2021). "Analysis of the future land use land cover changes in the gaborone dam catchment using ca-markov model: Implications on water resources."

 <u>Remote Sensing</u> 13(13): 2427.
 https://doi.org/10.3390/rs13132427.
- Nasiri, V., et al. (2022). "Land use and land cover mapping using Sentinel-2, Landsat-8 Satellite Images, and Google Earth Engine: A comparison of two composition methods." Remote Sensing 14(9): 1977. https://doi.org/10.3390/rs14091977.
- Pan, Y., et al. (2023). "A new change detection method for wetlands based on Bi-Temporal Semantic Reasoning UNet++ in Dongting Lake, China." <u>Ecological Indicators</u>

 155: 110997. https://doi.org/10.1016/j.ecolind.2023.110997.
- Pan, Y., et al. (2022). "Change detection of wetland restoration in China's Sanjiang National Nature Reserve using STANet method based on GF-1 and GF-6 images."

 <u>Ecological Indicators</u> **145**: 109612. https://doi.org/10.1016/j.ecolind.2022.109612.
- Rupasinghe, P. A. and P. Chow-Fraser (2024). "Change detection of wetland vegetation under contrasting water-level scenarios in coastal marshes of eastern Georgian Bay." <u>Landscape Ecology</u> **39**(3): 44. https://doi.org/10.1007/s10980-024-01829-9.
- Tabib Mahmoudi, F. and S. Hosseini (2021). "Three-dimensional building change detection using object-based image analysis (case study: Tehran)." <u>Applied Geomatics</u> **13**(3): 325-332. DOI: 10.1007/s12518-020-00349-w

- Talla, S., et al. (2019). "Multiclass Classification Using Random Forest Classifier." Int. J. Sci. Res. Comput. Sci. Eng. Inf. Technol 5(2): 493-496. https://doi.org/10.32628/CSEIT183821
- Teshager, Z. and K. Abeje (2021). "GIS and Remote Sensing based Land Us e/Land Cover Change Detection: The Case of Kility Watershed." J Remote Sens GIS 10(3).
- Tian, S., et al. (2016). "Random forest classification of wetland landcovers from multi-sensor data in the arid region of Xinjiang, China." Remote Sensing 8(11): 954. https://doi.org/10.3390/rs8110954.
- Toure, S. I., et al. (2018). "Land cover and land use change analysis using multi-spatial resolution data and object-based image analysis." Remote Sensing of Environment **210**: 259-268. https://doi.org/10.1016/j.rse.2018.03.023.
- Wingate, V. R., et al. (2016). "Mapping decadal land cover changes in the woodlands of north eastern Namibia from 1975 to 2014 using the Landsat satellite archived data."

 <u>Remote Sensing</u> **8**(8): 681. https://doi.org/10.3390/rs8080681.
- Zahir, I. L. M., et al. (2021). "Spatiotemporal land-use changes of Batticaloa municipal council in Sri Lanka from 1990 to 2030 Using Land Change Modeler." Geographies 1(3): 166-177. https://doi.org/10.3390/geographies1030010.
- Zhang, D.-D. and L. Zhang (2020). "Land cover change in the central region of the lower Yangtze River based on Landsat imagery and the Google Earth Engine: A case study in Nanjing, China." Sensors 20(7): 2091. https://doi.org/10.3390/s20072091.
- Zhang, Y., et al. (2021). <u>Research on wetland change detection based on Remote Sensing</u>. IOP Conference Series: Earth and Environmental Science, IOP Publishing. DOI: 10.1088/1755-1315/787/1/012061
- Zurqani, H. A., et al. (2018). "Geospatial analysis of land use change in the Savannah River Basin using Google Earth Engine." <u>International journal of applied earth observation and geoinformation</u> **69**: 175-185. DOI: 10.1016/j.jag.2017.12.006.